Journal of Magnetism and Magnetic Materials 446 (2018) 162–165

Contents lists available at ScienceDirect

Journal of Magnetism and Magnetic Materials

journal homepage: www.elsevier.com/locate/jmmm

Research articles

Near room-temperature magnetocaloric effect of Co-based bulk metallic glass

Cong Liu [a], Qiang Li [a,*], Juntao Huo [b,*], Weiming Yang [c], Liang Chang [a], Chuntao Chang [d], Yanfei Sun [a]

[a] School of Physics Science and Technology, Xinjiang University, Urumqi, Xinjiang 830046, People's Republic of China
[b] Ningbo Institute of Materials Technology & Engineering, Chinese Academy of Sciences, Ningbo, Zhejiang 315201, People's Republic of China
[c] School of Mechanics and Civil Engineering, State Key Laboratory for Geomechanics and Deep Underground Engineering, School of Sciences, China University of Mining and Technology, Xuzhou 221116, People's Republic of China
[d] School of Mechanical Engineering, Dongguan University of Technology, Dongguan 523808, People's Republic of China

ARTICLE INFO

Article history:
Received 28 June 2017
Received in revised form 26 August 2017
Accepted 1 September 2017
Available online 12 September 2017

Keywords:
Co-based bulk metallic glass
Magnetocaloric effect
Near room-temperature

ABSTRACT

$Co_{71}Mo_9P_{14}B_6$ bulk glassy rod with a maximum diameter of 4.5 mm is fabricated by combining fluxing treatment and J-quenching technique, and its magnetocaloric effect (MCE) has been investigated in the present work. The peak values of the magnetic entropy change and refrigerant capacity of the $Co_{71}Mo_9P_{14}B_6$ bulk metallic glass (BMG) are 0.96 J kg^{-1} K^{-1} and 70.5 J kg^{-1}, respectively, under a maximum applied field of 5 T. Most importantly, this BMG exhibits a Curie temperature of 317 K, which is suitable for room-temperature magnetic refrigeration. Combining the large glass-forming ability and near room-temperature MCE, the present $Co_{71}Mo_9P_{14}B_6$ BMG provides a candidate used as near room-temperature magnetic refrigerant.

1. Introduction

Compared with conventional gas compression/expansion refrigeration, magnetic refrigeration based on magnetocaloric effect (MCE) has attracted more attention for energy-efficient, environmentally friendly technological applications [1]. Up to now, the study of magnetic refrigeration materials has been mainly focused on crystalline intermetallic compounds, such as $Gd_5Si_2Ge_2$ [2], $LaFe_{11.4}Si_{1.6}$ [3], La-Ca-Mn-O [4], Ni-Mn-Sn [5], Mn-Fe-P-As [6]. They displayed giant MCE originating from the first order magneto-structural phase transition (FOMT). However, FOMT materials exhibit large hysteresis losses and mechanical instability upon magnetic field reversal, which limit their application of magnetic refrigeration [2]. Based on this reason, amorphous magnetocaloric materials with the second order magneto-structural phase transition (SOMT) are considered as alternative materials. SOMT materials show no structural transition at the Curie temperature (T_C), negligible hysteresis and broader operating temperature range. Furthermore, the disordered structure on an atomic scale of amorphous alloys reduces thermal conductivity and keeps a higher electrical resistivity, which is benefit to minimize the thermal conduction and eddy current losses [7]. Therefore, amorphous alloys are considered to be the optimal candidates for magnetic refrigeration materials. Amorphous alloys used for magnetic refrigeration can be divided into two classes, namely, RE-based and TM-based amorphous alloys. RE-based amorphous alloys exhibit the large magnetic entropy change ΔS_M and the extremely low T_C, which is suitable for low temperature magnetic refrigeration [8–10]. Compared with RE-based amorphous alloys, TM-based amorphous alloys generally exhibit low value of ΔS_M. However, TM-based amorphous alloys show lower materials cost and higher corrosion resistance regarding to RE-based metals. More importantly, TM-based amorphous alloys have generally a high magnetic transition temperature, which can be easily tuned to be near room-temperature [11]. Room-temperature magnetocaloric materials can be used for domestic refrigerators, air conditions and other refrigeration devices, and thus has great practical value and research significance.

The recent study on the MCE of TM-based amorphous alloys is mainly focused on Fe-based amorphous alloys and there are few works on the MCE of Co-based amorphous alloys. Additionally, at present the study on the MCE of amorphous alloys is mainly focused on amorphous ribbons. However, bulk metallic glasses (BMGs) can be made into the final required shapes to achieve maximize efficient heat transfer between magnetic refrigerants and heat-exchange medium regarding to amorphous ribbons [12,13]. Therefore it is of great significance to develop magnetocaloric BMGs. More recently, we have successfully fabricated quaternary $Co_{71}Mo_9P_{14}B_6$ BMG with a maximum diameter of 4.5 mm by

* Corresponding authors.
E-mail addresses: qli@xju.edu.cn (Q. Li), huojuntao@nimte.ac.cn (J. Huo).

http://dx.doi.org/10.1016/j.jmmm.2017.09.026

combining fluxing treatment and J-quenching technique [14]. In this work, we further investigate the MCE of the $Co_{71}Mo_9P_{14}B_6$ BMG. It is of great interest that this BMG exhibits a near room-temperature MCE. This work is expected to inspire further research on amorphous MCE materials as room-temperature magnetic refrigeration.

2. Experimental

The mother alloy ingots of $Co_{71}Mo_9P_{14}B_6$ were prepared by torch-melting a mixture of pure Co powders (99 mass%), Mo powders (99.9 mass%), Co_2P powders (98 mass%), and B pieces (99.95 mass%) under a high-purity argon atmosphere. Subsequently, the mother alloy ingots were fluxed in a fluxing agent at an elevated temperature for 4 h under the vacuum corresponding to a residual of ~50 Pa. The fluxing agent is prepared by mixing B_2O_3 and CaO with a mass ratio of 3:1. After fluxing treatment, the alloy ingots were cooled down to room-temperature and then were subjected to J-quenching technique, the details of which can be found elsewhere [14]. As a result, $Co_{71}Mo_9P_{14}B_6$ alloy rod specimens with diameters of 1.0–4.5 mm and lengths of a few centimeters were prepared.

The amorphous nature of the as-prepared specimens was checked by X-ray diffractometer (XRD) using Cu K_α radiation. The thermal behavior of the as-prepared specimens was examined by differential scanning calorimetry (DSC, NETZSCH DSC 404F1) at a heating rate of 0.33 K/s under an Ar atmosphere. The temperature and field dependences of the magnetization were measured using a SQUID magnetometer (MPMS, Quantum Design®).

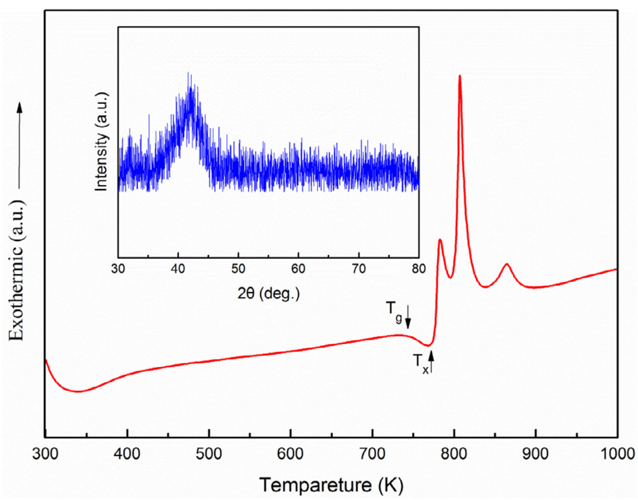

Fig. 1. XRD and DSC curves of $Co_{71}Mo_9P_{14}B_6$ BMG.

3. Results and discussion

Fig. 1 shows the XRD pattern and DSC curve of the as-prepared $Co_{71}Mo_9P_{14}B_6$ BMG with a diameter of 4.5 mm. The XRD pattern of the specimen reveals a typical broad diffraction peak and no crystalline peaks, illustrating the fully glassy phase formation. The DSC curve of the specimen shows obvious endothermic glass transition behaviors and exothermic crystallization peaks. The value of the glass transition temperature (T_g), the crystallization temperature (T_x) and the value of the total crystallization enthalpy ΔH_x of the specimen are 743 K, 770 K and 126.4 J g^{-1}, respectively. The DSC result further confirms the fully glassy structure of the present specimen.

Fig. 2 shows the temperature dependence of the magnetization and dM/dT versus temperature curves for $Co_{71}Mo_9P_{14}B_6$ BMG under 0.02 T. The Curie temperature (T_C) of this BMG is 317 K determined from the differentiation of M-T curve as shown in the inset of Fig. 2, which is near room-temperature. The isothermal magnetization curves of $Co_{71}Mo_9P_{14}B_6$ BMG under various applied fields up to 5 T in the temperature range of 245–400 K are displayed in Fig. 3(a). The magnetization saturates is achieved at low applied magnetic fields below the T_C, indicating a low number density of domain-wall pinning site in the present Co-based BMG. The M-H curves become linear with the temperature increasing near and above T_C, indicating the transitions from ferromagnetic

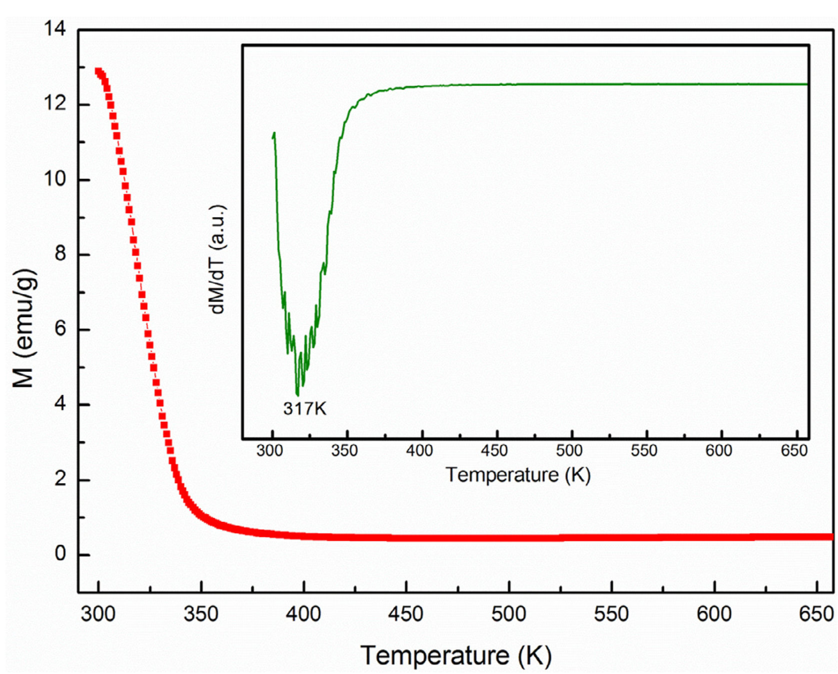

Fig. 2. Temperature dependence of the magnetization and dM/dT versus temperature curves for $Co_{71}Mo_9P_{14}B_6$ BMG under 0.02 T.

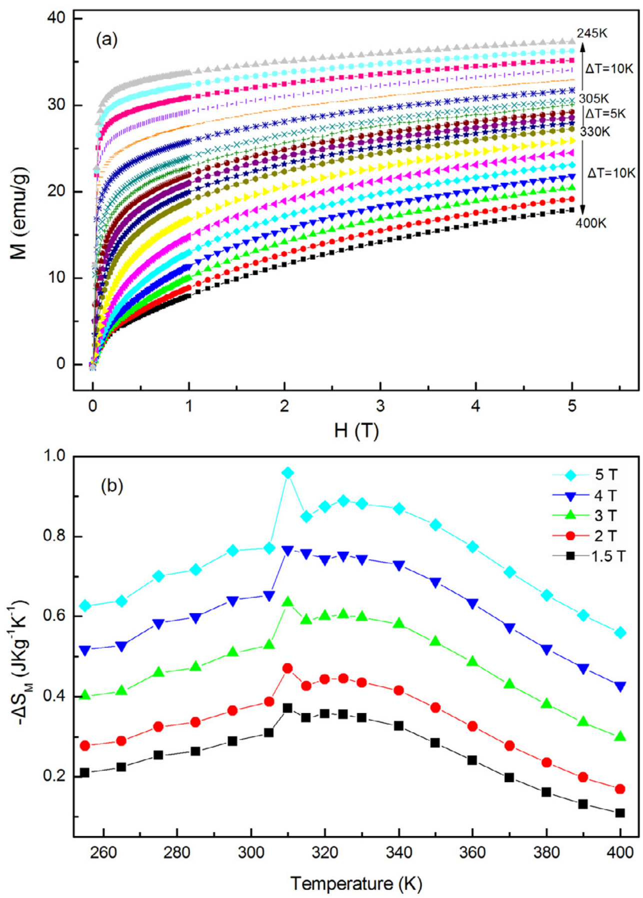

Fig. 3. (a) Isothermal magnetization curves of $Co_{71}Mo_9P_{14}B_6$ BMG measured at temperatures between 245 and 400 K. (b) Magnetic entropy changes as a function of temperature under 1.5–5 T for $Co_{71}Mo_9P_{14}B_6$ BMG.

state to paramagnetic state [15]. The MCE is quantified by a magnetic entropy change (ΔS_M), which can be calculated from magnetization isotherms using the Maxwell relation [16]:

$$\Delta S_M(T,H) = \int_0^{H_{max}} \left(\frac{\partial M}{\partial T}\right)_H dH \tag{1}$$

where H_{max} is the maximum applied field. In practice, an alternative formula is generally used for numerical calculation:

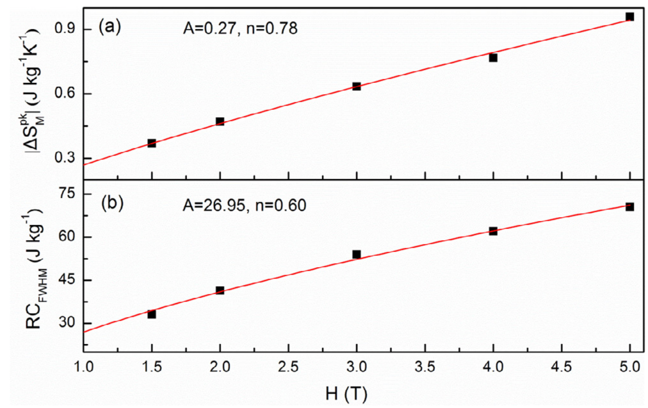

Fig. 4. Magnetic field dependence of the (a) maximum magnetic entropy changes $|\Delta S_M^{pk}|$, (b) RC_{FWHM} for $Co_{71}Mo_9P_{14}B_6$ BMG.

$$\Delta S_M(T_i,H) = \frac{\int_0^H M(T_i,H)dH - \int_0^H M(T_{i+1},H)dH}{T_i - T_{i+1}} \tag{2}$$

Fig. 3(b) shows the temperature dependence of $-\Delta S_M$ of $Co_{71}Mo_9P_{14}B_6$ BMG under 1.5–5 T calculated by Eq. (2). The curves under the different applied fields of Fig. 3(b) show two peaks, of which one is a sharp peak near 310 K and another one is a broad diffuse peak near 325 K. The presence of two peaks in the magnetic entropy change curves may be caused by coexistence of the magnetic transition and spin reorientation transition when the applied magnetic field is larger than the spin reorientation field of the present Co-based system [13,17]. Additionally, it can be found that the peak temperature (T_{peak}) of the ΔS_M curves BMG is lower than the T_C for the present Co-based, which may be due to inhomogeneities in the studied sample [18,19]. The peak value of ΔS_M ($|\Delta S_M^{pk}|$) is 0.37 J kg^{-1} K^{-1} under 1.5 T and 0.96 J kg^{-1} K^{-1} under 5 T, respectively, and is listed in Table 1. In comparison, the MCE properties and the GFA of some selected Fe-based and Co-based amorphous alloys are also listed in Table 1. It can be seen that the $|\Delta S_M^{pk}|$ value of the present $Co_{71}Mo_9P_{14}B_6$ BMG is close to that of $Co_{62}Nb_6Zr_2B_{30}$ glassy ribbon, but lower than that of all Fe-based amorphous alloys. The lower $|\Delta S_M^{pk}|$ value of the present Co-based BMG may attribute to the anti-ferromagnetic coupling between the magnetic moments of Co and Mo atoms. The *RC* is another relevant parameter to characterize the efficiency of magnetic refrigerant. The *RC* is calculated by the peak entropy change $|\Delta S_M^{pk}|$ and the full width at

Table 1
The maximum diameter for fully glass formation (D_{max}) and magnetocaloric properties under an applied field of 1.5 T, 2 T and 5 T for some selected Co-based and Fe-based glassy alloys. Here C stands for crystal.

Composition (at%)	D_{max} (mm)	T_C (K)	$-\Delta S_M$ (J kg^{-1} K^{-1})			RC_{FWHM} (J kg^{-1})			Refs.
			1.5 T	2 T	5 T	1.5 T	2 T	5 T	
$Co_{71}Mo_9P_{14}B_6$	4.5	317	0.37	0.47	0.96	33.0	41.3	70.5	This work
$Co_{62}Nb_6Zr_2B_{30}$		210	0.36						[24]
$Co_{40.2}Fe_{20.1}Ni_{6.7}B_{22.7}Si_{5.3}Nb_5$		462	0.62	0.73			124.1		[15]
$Fe_{80}P_{13}C_7$	2	579	2.20	2.7	5.05	125.6	170.1	479.8	[13]
$Fe_{79}Gd_1B_{12}Cr_8$		355	1.42	3.59		153		627	[19]
$Fe_{80}B_{10}Zr_9Cu_1$		356		1.72	3.28		141.4	444.8	[25]
$Fe_{77}Ni_3B_{10}Zr_9Cu_1$		385		1.61	3.13		119.3	392.5	[25]
$Fe_{77}Ta_5B_{10}Zr_9Cu_1$		313		1.04	2.03		92.2	241.5	[25]
$(Fe_{0.59}Tm_{0.17}B_{0.24})_{96}Nb_4$		316	0.91			59			[11]
$Fe_{66}Mn_{14}P_{10}B_7C_3$		319	0.91	1.12		99.84	134.25		[26]
Gd (C)		294		5.5			214.5		[27]
$MnFeP_{0.45}As_{0.55}$ (C)		305		14.5	18		152.25		[6]
$Gd_5Si_2Ge_2$ (C)		275		14	18.5		109.2		[2]

half maximum δT_{FWHM} of the $|\Delta S_M|$ peak [20]. The RC_{FWHM} values of the present Co-based BMG are about 33.0 J kg^{-1} under 1.5 T and 70.5 J kg^{-1} under 5 T, respectively.

Fig. 4 shows the magnetic field dependence of $\left|\Delta S_M^{pk}\right|$ and RC_{FWHM} for the specimen. According to the mean field theory, $\left|\Delta S_M^{pk}\right|$ and RC_{FWHM} can be expressed approximately as $\Delta S_M^{pk} \propto AH^n$ and $RC \propto BH^N$, respectively [21]. The exponent n and N, controlled by the critical exponents of $Co_{71}Mo_9P_{14}B_6$ BMG, can be extracted through fitting the experimental data in Fig. 4(a) and (b) with the relations above. The value of the exponent n is 0.78 here, which is larger than the that (=2/3) of n predicted by the mean field theory [22], meaning that the fluctuations and heterogeneities in magnetic microstructures exist in the present specimen [23].

4. Conclusions

$Co_{71}Mo_9P_{14}B_6$ BMG with a maximum diameter of 4.5 mm has been prepared by combining fluxing treatment and J-quenching technique. The present $Co_{71}Mo_9P_{14}B_6$ BMG does not exhibit a high MCE, of which the peak value of $|\Delta S_M|$ is 0.37 J kg^{-1} K^{-1} under 1.5 T and 0.96 J kg^{-1} K^{-1} under 5 T, respectively, and the value of RC_{FWHM} is about 33.0 J kg^{-1} under 1.5 T and 70.5 J kg^{-1} under 5 T, respectively. But it is of great significance that the Curie temperature of the present Co-based BMG is 317 K, exhibiting near room-temperature MCE. Therefore, the combination of near room-temperature MCE and the large GFA make the present $Co_{71}Mo_9P_{14}B_6$ BMG a potential material for room-temperature refrigeration.

Acknowledgement

This research was sponsored by the Natural Science Foundation of Xinjiang Uyghur Autonomous Region (No. 2016D01C052).

Appendix A. Supplementary data

Supplementary data associated with this article can be found, in the online version, at http://dx.doi.org/10.1016/j.jmmm.2017.09.026.

References

[1] O. Gutfleisch, M.A. Willard, E. Brück, C.H. Chen, S.G. Sankar, J.P. Liu, Magnetic materials and devices for the 21st century: stronger lighter, and more energy efficient, Adv. Mater. 23 (2011) 821–842.
[2] V.K. Pecharsky, K.A. Gschneidner Jr., Giant magnetocaloric effect in $Gd_5(Si_2Ge_2)$, Phys. Rev. Lett. 78 (1997) 4494–4497.
[3] F. Hu, B. Shen, J. Sun, Z. Cheng, Influence of negative lattice expansion and metamagnetic transition on magnetic entropy change in the compound $LaFe_{11.4}Si_{1.6}$, Appl. Phys. Lett. 78 (2001) 3675–3677.
[4] Z.B. Guo, Y.W. Du, J.S. Zhu, H. Huang, W.P. Ding, D. Feng, Large magnetic entropy change in perovskite-type manganese oxides, Phys. Rev. Lett. 78 (1997) 1142–1145.
[5] T. Krenke, E. Duman, M. Acet, E.F. Wassermann, X. Moya, L. Mañosa, A. Planes, Inverse magnetocaloric effect in ferromagnetic Ni-Mn-Sn alloys, Nat. Mater. 4 (2005) 450–454.
[6] O. Tegus, E. Brück, K.H.J. Buschow, F.R.D. Boer, Transition-metal-based magnetic refrigerants for room-temperature applications, Nature 415 (2002) 150–152.
[7] E.P. Nóbrega, A. Caldas, P.O. Ribeiro, B.P. Alho, T.S.T. Alvarenga, V.S.R. de Sousa, N.A. de Oliveira, P.J. von Ranke, Theoretical investigation on the magnetocaloric effect in amorphous systems, application to: $Gd_{80}Au_{20}$ and $Gd_{70}Ni_{30}$, J. Appl. Phys. 113 (2013) 243903.
[8] X.Y. Liu, J.A. Barclay, R.B. Gopal, M. Földeàki, R. Chahine, T.K. Bose, P.J. Schurer, J.L. LaCombe, Thermomagnetic properties of amorphous rare-earth alloys with Fe Ni, or Co, J. Appl. Phys. 79 (1996) 1630–1641.
[9] J. Li, J.Y. Law, H. Ma, A. He, Q. Man, H. Men, J. Huo, C. Chang, X. Wang, R.-W. Li, Magnetocaloric effect in Fe-Tm-B-Nb metallic glasses near room temperature, J. Non-Cryst. Solids 425 (2015) 114–117.
[10] F.X. Qin, N.S. Bingham, H. Wang, H.X. Peng, J.F. Sun, V. Franco, S.C. Yu, H. Srikanth, M.H. Phan, Mechanical and magnetocaloric properties of Gd-based amorphous microwires fabricated by melt-extraction, Acta Mater. 61 (2013) 1284–1293.
[11] Y.F. Wang, F.X. Qin, Y.H. Wang, H. Wang, R. Das, M.H. Phan, H.X. Peng, Magnetocaloric effect of Gd-based microwires from binary to quaternary system, AIP Adv. 7 (2017) 056422.
[12] A. Smith, C.R.H. Bahl, R. Bjørk, K. Engelbrecht, K.K. Nielsen, N. Pryds, Materials challenges for high performance magnetocaloric refrigeration devices, Adv. Energy Mater. 2 (2012) 1288–1318.
[13] W. Yang, J. Huo, H. Liu, J. Li, L. Song, Q. Li, L. Xue, B. Shen, A. Inoue, Extraordinary magnetocaloric effect of Fe-based bulk glassy rods by combining fluxing treatment and J-quenching technique, J. Alloy. Compd. 684 (2016) 29–33.
[14] L. Bie, Q. Li, D. Cao, H. Li, J. Zhang, C. Chang, Y. Sun, Preparation and properties of quaternary CoMoPB bulk metallic glasses, Intermetallics 71 (2016) 7–11.
[15] I. Kucuk, K. Sarlar, A. Adam, E. Civan, Magnetocaloric and magnetoresistance properties in Co based $(Co_{0.402}Fe_{0.201}Ni_{0.067}B_{0.227}Si_{0.053}Nb_{0.05})_{100-x}Cu_x$(x =0-1) glassy alloys, Philos. Mag. 96 (2016) 3120–3130.
[16] T. Hashimoto, T. Numasawa, M. Shino, T. Okad, Magnetic refrigeration in the temperature range from 10 K to room temperature: the ferromagnetic refrigerants, Cryogenics 21 (1981) 647–653.
[17] M. Shao, S. Cao, Y. Wang, S. Yuan, B. Kang, J. Zhang, Large magnetocaloric effect in $HoFeO_3$ single crystal, Solid State Commun. 152 (2012) 947–950.
[18] V. Franco, A. Conde, M.D. Kuz'min, J.M. Romero-Enrique, The magnetocaloric effect in materials with a second order phase transition: Are T_C and T_{peak} necessarily coincident?, J Appl. Phys. 105 (2009) 07A917.
[19] M.D. Kuz'min, M. Richter, A.M. Tishin, Field dependence of magnetic entropy change: whence comes an intercept?, J Magn. Magn. Mater. 321 (2009) L1–L3.
[20] K.A. Gschneidner Jr., V.K. Pecharsky, Magnetocaloric materials, Annu. Rev. Mater. Sci. 30 (2000) 387–429.
[21] J.Y. Law, R.V. Ramanujan, V. Franco, Tunable Curie temperatures in Gd alloyed Fe-B-Cr magnetocaloric materials, J. Alloy. Compd. 508 (2010) 14–19.
[22] H. Oesterreicher, F.T. Parker, Magnemagnetic cooling near Curie temperatures above 300 K, J. Appl. Phys. 55 (1984) 4334–4338.
[23] J. Huo, L. Huo, J. Li, H. Men, X. Wang, A. Inoue, C. Chang, J.-Q. Wang, R.-W. Li, High-entropy bulk metallic glasses as promising magnetic refrigerants, J. Appl. Phys. 117 (2015) 073902.
[24] L.M. Moreno, J.S. Blázquez, J.J. Ipus, J.M. Borrego, V. Franco, A. Conde, Magnetocaloric effect of $Co_{62}Nb_6Zr_2B_{30}$ amorphous alloys obtained by mechanical alloying or rapid quenching, J. Appl. Phys. 115 (2014) 17A302.
[25] X.C. Zhong, H.C. Tian, S.S. Wang, Z.W. Liu, Z.G. Zheng, D.C. Zeng, Thermal, magnetic and magnetocaloric properties of $Fe_{80-x}M_xB_{10}Zr_9Cu_1$ (M=Ni, Ta; x=0, 3, 5) amorphous alloys, J. Alloy. Compd. 633 (2015) 188–193.
[26] H. Zhang, R. Li, T. Xu, F. Liu, T. Zhang, Near room-temperature magnetocaloric effect in FeMnPBC metallic glasses with tunable Curie temperature, J. Magn. Magn. Mater. 347 (2013) 131–135.
[27] V.K. Pecharsky, K.A. Gschneidner Jr., Magnetic phase transitions and the magnetothermal properties of gadolinium, Phys. Rev. B 57 (1998) 3478–3491.